Dual Refractive Index and Viscosity Sensing Using Polymeric Nanofibers Optical Structures

Salvador Ponce-Alcántara, David Martín-Sánchez, Miroslavna Kovylina, Ana Pérez-Márquez, Jon Maudes, Nieves Murillo, and Jaime García-Rupérez, *Senior Member, IEEE*

***Abstract*— Porous materials have demonstrated to be ideal candidates for the creation of optical sensors with very high sensitivities. This is due both to the possibility of infiltrating the target substances into them and to their notable surface-to-volume ratio that provides a larger biosensing area. Among porous structures, polymeric nanofibers (NFs) layers fabricated by electrospinning have emerged as a very promising alternative for the creation of low-cost and easy-to-produce high performance optical sensors, for example, based on Fabry-Pérot (FP) interferometers. However, the sensing performance of these polymeric NFs sensors is limited by the low refractive index contrast between the NFs porous structure and the target medium when performing in-liquid sensing experiments, which determines a very low amplitude of the FP interference fringes appearing in the spectrum. This problem has been solved with the deposition of a thin metal layer (∼ 3 nm) over the NFs sensing layer. We have successfully used these metal-coated FP NFs sensors to perform several real-time and in-flow refractive index sensing experiments. From these sensing experiments, we have also determined that the sponge-like structure of the NFs layer suffers an expansion/compression process that is dependent of the viscosity of the analyzed sample, what thus gives the possibility to perform a simultaneous dual sensing of refractive index and viscosity of a fluid.**

***Index Terms*— Fabry-Perot, nanofibers layer, Nanophotonics, polymers, porous structure, real-time sensor, refractive index, viscosity.**

I. Introduction

NOWADAYS, sensors are used almost everywhere, as in industrial machinery and process control, building management, wearable and communications devices, environmental monitoring, medical diagnosis or biological/chemical threats detection, among many other fields. They are designed to perform measurements based on different transduction mechanisms: physical, chemical, optical, mechanical and electromagnetic. Particularly, the use of optical sensors provides important advantages compared to other transduction technologies, as for example, high sensitivity, high degree of miniaturization, shorter time to result, label-free detection, requirement of very low volumes of sample and reagents, resistance to hazardous and harsh environments, and immunity to electromagnetic interferences [1].

Optical sensors based on the measurement of refractive index changes are widely applied to the detection of substances/analytes in many fields such as clinical diagnosis, pharmaceutical and drug analysis, pollution monitoring or food control [2] – [6]. Most optical sensors use the interaction of the evanescent field of a guided mode with the surrounding media to perform the sensing [7], [8]. However, since only that lower-intensity evanescent field propagating outside the optical structure is used for sensing purposes, the maximum achievable sensitivity is significantly limited. In order to overcome this limitation and to use the higher-intensity optical field located inside the structure for sensing purposes, there is an increasing interest in using porous materials for the development of optical sensing structures [9] – [11]. Additionally, porous materials also provide an extremely high internal surface where a huge amount of biorecognition probes can be immobilized in order to perform a selective detection of increased quantity of analytes, which is also translated into an increase of the sensitivity.

In the present study, we report our results on the development of porous optical sensors based on polymeric nanofibers (NFs) layers deposited by electrospinning. Polymeric NFs layers exhibit many interesting properties that makes them ideal candidates to build sensing structures, as for example, a high surface-to-volume ratio (of the order of 290 m^2/cm^3), a high porosity (up to 90%), an adjustable pore size, a sponge-like configuration for a better sample infiltration, a low production cost and the possibility to be manufactured over large areas [12], [13], among others. Because of that, electrospun NFs layers are increasingly used for the development of different types of sensors, typically based on non-optical transduction mechanisms [14], like amperometric [15], electrochemical [16], in the elaboration of improved Enzyme-Linked Immunosorbent Assays (ELISAs) [17], and in advanced point-of-care devices [18]. Our group has recently demonstrated how a NFs layer can be used as a high sensitivity Fabry-Pérot (FP) photonic sensor by performing static sensing tests [19]. However, problems were observed when performing real-time and in-flow dynamic measurements, mainly due to the low refractive index contrast between the NFs polymeric

Manuscript received July 26, 2019; accepted August 26, 2019. Date of publication September 2, 2019; date of current version November 26, 2019. This work was supported by the Spanish government through the project TEC2015-63838-C3-1-R-OPTONANOSENS and from the Basque government through the KK-2019/00101-μ4FINDUSTRY. The associate editor coordinating the review of this article and approving it for publication was Dr. Ioannis Raptis. *(Corresponding author: Salvador Ponce-Alcántara.)*

S. Ponce-Alcántara, D. Martín-Sánchez, M. Kovylina, and J. García-Rupérez are with the Nanophotonics Technology Center, Universitat Politècnica de València, 46022 Valencia, Spain (e-mail: salponce@ntc.upv.es; damarsa5@ntc.upv.es; mikov@ntc.upv.es; jaigarru@ntc.upv.es).

A. Pérez-Márquez, J. Maudes, and N. Murillo are with the TECNALIA Research & Innovation, 20009 Donostia-San Sebastián, Spain (e-mail: ana.perez@tecnalia.com; jon.maudes@tecnalia.com; nieves.murillo@tecnalia.com).

Digital Object Identifier 10.1109/JSEN.2019.2938832

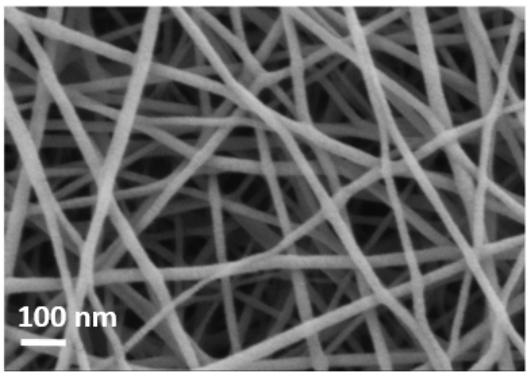

Fig. 1. FESEM image of a typical NFs layer used in this study.

material and the target medium. In this work, we have solved this problem by depositing a thin metal layer over the NFs layer in order to increase the amplitude of the FP fringes. Several alternatives have been studied in order to determine the best metal to be used and its optimal thickness, being able to obtain an improvement of up to 70% when using a 3 nm gold film. These metal-coated FP NFs sensors have been used to perform refractive index sensing experiments where different concentrations of ethanol (EtOH) in deionized water (DIW) were flowed over the sensor. Sensitivities determined from these experiments were significantly higher than those theoretically expected and they were different depending on the EtOH concentration. From these results, we have determined that the FP NFs sensor is not only sensitive to refractive index variations, but also to changes in the viscosity of the liquid, which produces an expansion/compression of the sponge-like structure of the NFs layer during the flow of the target samples.

II. Nanofibers Layers as Optical Sensors

Porous optical sensors have been built from polymeric NFs layers created by electrospinning process. These layers have been deposited over a polished silicon wafer, and act as a Fabry-Pérot (FP) interferometer. NFs layers with average diameters between 22 and 40 nm and high porosities have been achieved with a electrospinning solution realized with a 6 wt% of polyamide 6 (PA6) and 5 wt% of pyridine salt. Further details about the fabrication process are provided in reference [19]. Fig. 1 shows a Field Emission Scanning Electron Microscope (FESEM) (Zeiss Ultra 55) image of a typical NFs layer used in this study.

The FP interferometer configuration has been selected due to the good relationship between fabrication complexity, cost, and sensitivity [20]. This type of optical sensing structure has a reflectance spectrum characterized by the presence of interference fringes, as a result of the constructive and destructive interferences produced by the light reflected at the interfaces between the NFs layer, the top medium and the silicon substrate, as schematically depicted in Fig. 2(a). The position of these FP interference will shift depending on the refractive index of the fluids filling the NFs layer, leading to the sensing behavior. Representative reflectance spectra in the visible (VIS) and near infrared (NIR) regions of a typical NFs layer deposited on a polished silicon

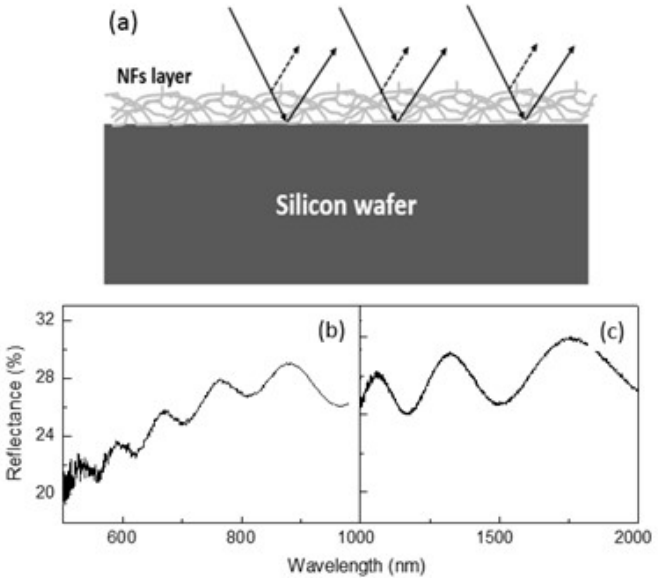

Fig. 2. (a) Schematic diagram of a FP NFs interferometer. Specular reflectance measurement in the (b) VIS and (c) NIR ranges of the spectrum for a NFs layer fabricated with 6 wt% of PA6 and 5 wt% of pyridine. Spectra have been measured using a Fourier-Transform Infrared Spectroscope (FTIR) (Bruker VERTEX 80) with a resolution of 4 cm^{-1} and 12 averaged scans.

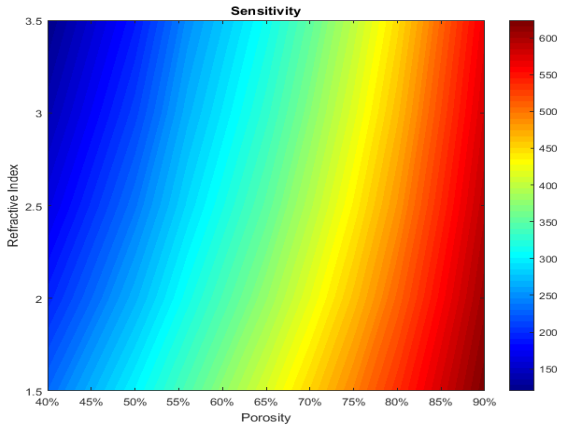

Fig. 3. Theoretical sensitivity in the visible range of the spectrum of a porous FP sensing layer (in nm/RIU) as a function of the refractive index of the bulk material (n_{bulk} from 1.5 to 3.5) for different porosities (P from 40% to 90%).

wafer are represented in Fig. 2(b) and Fig. 2(c), respectively. The Transfer Matrix Method (TMM) [21] has been used to estimate the refractive index and the thickness of the NFs porous samples from reflectance measurements. Values close to 1.22 and 1150 nm have been obtained for these parameters, respectively.

III. Dependence of the Sensitivity With the Porosity of a Sensing Structure

Simulations based on the effective medium model given by Looyenga [22] have been done in order to estimate the sensitivity in the visible range of the spectrum of a FP structure, depending on the refractive index of the bulk material and on the porosity. Reference [19] shows more details about these simulations. Fig. 3 represents the trends

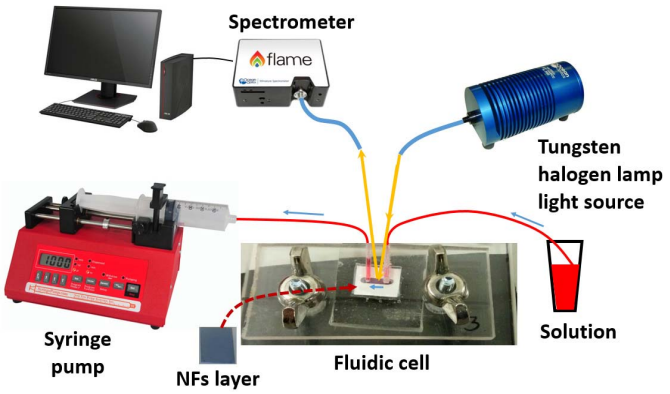

Fig. 4. Scheme of the opto-fluidic setup used to carry out the real-time and in-flow sensing experiments.

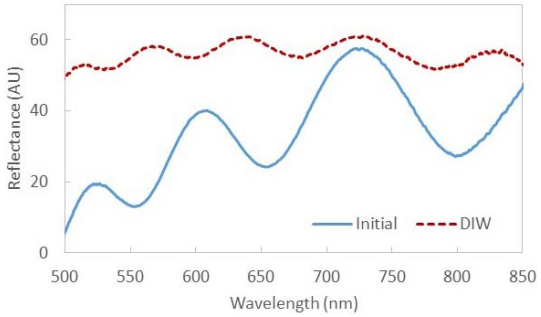

Fig. 5. Reflectance spectrum of an as-fabricated PA6 NFs FP layer in air (labelled as "Initial") and when DIW is flowed.

on the sensitivity. For the calculations, the optical thickness (i.e. refractive index $\times$ thickness) of the porous layer has been properly selected to have a maximum fringe located close to 700 nm, whose shift has been measured to determine the sensitivity. According to these simulation results, the porosity of the sensor has a crucial importance on the sensitivity, since higher porosities imply that a higher volume of the structure will change its refractive index when the sensing process is carried out. Besides, the refractive index of the bulk material (n_{bulk}) has also a large influence on the sensitivity of the porous FP sensing layer. In this respect, higher sensitivities can be obtained for porous FP sensing layers fabricated with lower refractive index bulk materials.

IV. Experimental Setup

According to previous studies in our research group based on real-time sensing measurements with porous silicon sensors [11], a fluidic cell has been designed to analyze the sensitivity of a FP sensing structure made of NFs layers. Fig. 4 shows a scheme of the opto-fluidic setup used for the experiments.

The NFs layer to be characterized is placed between two transparent methacrylate pieces. In order to flow different solutions over the sensor, a 1 cm^2 adhesive tape with a 0.3 $\times$ 2.0 $\times$ 7.0 mm (height $\times$ width $\times$ length) channel defined on its center has been fixed to the upper methacrylate piece. Fluids are introduced to and extracted from the channel through the fluidic tubes connected to the solution to be analyzed in one side, and to a syringe pump on the other side. The pump has been configured in withdraw mode in order to generate the vacuum necessary to suck the solutions from the vial located at the end of the microfluidic system. The pump has been set to a constant flow rate of 20 μL/min during the whole experiment.

A tungsten halogen lamp light source has been used to illuminate the sample. The reflected light has been analyzed in real-time with a VIS-NIR spectrometer (Ocean Optics - Flame T). The wavelength range for reflectance measurements has been from 500 to 900 nm with a resolution of 215 pm. Four consecutive spectra were measured every 2 ms and averaged to provide the final result. The optical fibers from the light source and to the spectrometer have been placed with an angle of 15° respect the perpendicular axis of the NFs layer.

V. Improvement of FP Spectrum Using Metal Layers

When trying to perform real-time sensing measurements using the FP NFs sensor presented in chapter II, a significant worsening of the spectral response was observed when flowing DIW over the sensor. As it can be observed in Fig. 5, the amplitude of the FP fringes (i.e., the difference between maximum and minimum reflectance values) has a notable reduction due to the low index contrast between the NFs layer filled with DIW and the medium itself (DIW).

In order to overcome this problem, a thin metal layer has been deposited over the NFs structure. Noble metals have been selected due to their high reflectance, improved hardness (compared to NFs) and a high oxidation potential suitable for sensing in aqueous media. Three different metals have been studied: gold (Au), silver (Ag) and platinum (Pt).

Simulations have been done in order to estimate the optical effect of the metal layer deposition on the final reflectance of a NFs structure. The goal is to get minimum reflectance values close to zero and high amplitudes of the interference fringes. Additionally, the final average diameter (i.e., NF + metal layer) has to be small enough in order to have an adequate optical response. Optical simulations based on TMM have been done considering a two-layer structure. The first layer, corresponding to the NFs, is in contact with the silicon wafer and has a refractive index of 1.22 and a thickness of 1150 nm. These values are the average ones obtained in different electrospinning processes. The second layer models the metal deposited on top of the previous one, whose thickness has been changed from 1 to 8 nm. The results for the maximum and minimum reflectance values as well as their difference in the range from 600 to 700 nm are shown in Fig. 6(a), (b), and (c), respectively.

The maximum reflectance value increases very quickly with thickness for all metals, especially in the case of Au and Ag (Fig. 6(a)). Meanwhile, the minimum reflectance (Fig. 6(b)) is non-linear with thickness, exhibiting a minimum around 2 nm for Pt and around 5 nm for Ag and Au. Finally, this determines the non-linear increase for the difference between maximum and minimum of reflectance (Fig. 6(c)). According to [23], for higher metal thicknesses, deposited layers tend to behave as a

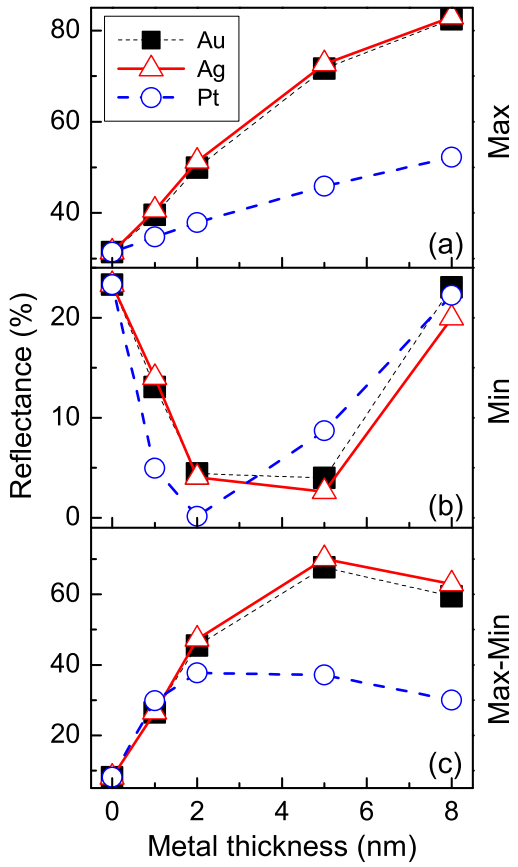

Fig. 6. TMM simulations of the effect of a thin metal layer deposited on top of the NFs structure for: gold (Au, black squares), silver (Ag, red triangles), and platinum (Pt, blue circles). Maximum-minimum differences have been calculated in the range from 600 to 700 nm.

metal mirror, providing in our case high minimum reflectance values and lower maximum-minimum differences.

Experimentally, gold and platinum layers have been achieved by sputtering deposition, while silver layers have been obtained by electron beam evaporation. Besides on the samples having the NFs layers, metals have also been deposited on reference samples of silicon dioxide for their physical characterization using atomic force microscopy (AFM). Fig. 7 shows the effect on the experimental reflectance spectrum after Au deposition on the NFs layer. The results are similar to those obtained in the simulations: for low thicknesses ($\sim$ 1 nm), the effect of the metal on the reflectance is not very significant. For high thicknesses ($\geq$ 6 nm), the specular reflectance of the metal layer introduces an offset into the reflectance. For intermediate thicknesses ($\sim$ 3 nm), an optimal reflectance is achieved. Therefore, in the present study metal thicknesses of $\sim$ 3 nm have been used to improve the amplitude of the FP fringes of the fabricated PA6 FP NFs sensor. Fig. 8 shows the experimental reflectance of different NFs layers with a gold, silver or platinum layer of $\sim$ 3 nm. Minimum values close to zero have been obtained in all of them; the highest maximum values have been achieved with silver and gold.

Finally, a significant signal improvement has been observed during the DIW flowing sensing experiments. As it is depicted in Fig. 9, the spectral FP fringes can be clearly distinguished

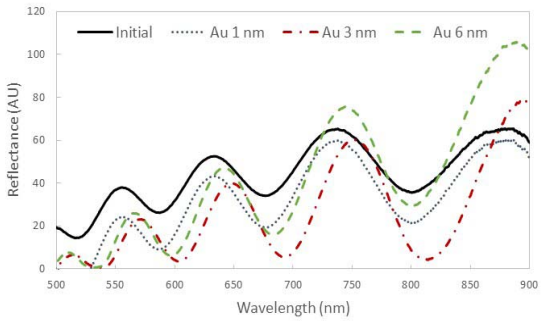

Fig. 7. Effect of the metal thickness on the reflectance spectrum of a NFs layer. Three gold thicknesses are shown: 1, 3 and 6 nm (blue dot, red dash-dot and green dash, respectively). The black reflectance corresponds to the NFs layer without any metal.

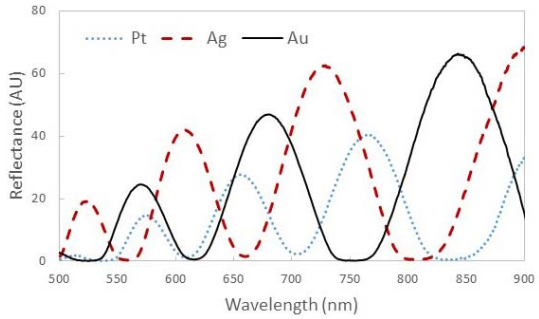

Fig. 8. Experimental reflectance spectra of different NFs layers with a deposited platinum, silver or gold layer (blue dot, red dash and black line, respectively), with an average thickness of 3 nm.

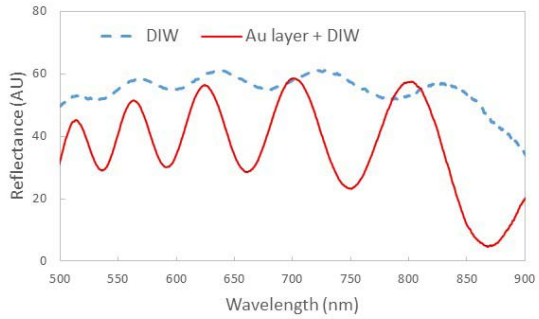

Fig. 9. Reflectance spectrum of a NFs layer without and with a thin ($\sim$ 3 nm) gold layer during a DIW flowing test.

compared to the low maximum-minimum difference observed for the bare NFs layer.

Accordingly, a NFs structure with a 3 nm thick gold layer deposited on top has been used in the subsequent experiments. Gold has been selected instead silver due to its easier and faster deposition method using our laboratory equipment.

VI. Sensing Experiments and Discussion

A NFs layer with a thickness of 1110 nm, an effective refractive index of 1.25 and with a $\sim$ 3 nm thick gold layer has been used to determine the sensitivity of this kind of sensors in real-time and in-flow. The porosity of the NFs layer has been estimated with the Looyenga model [22], giving values close to 60%. Three sensing test flowing different concentrations of

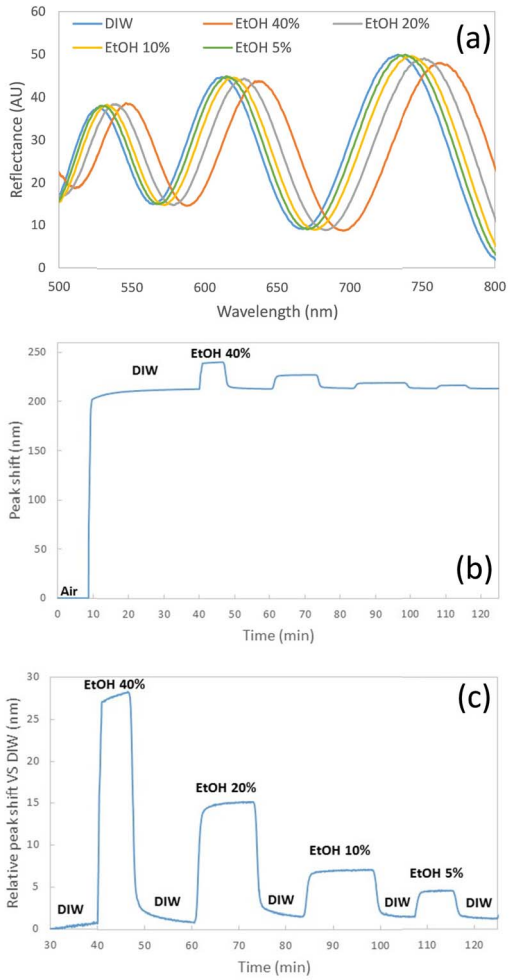

Fig. 10. (a) Reflectance spectrum of the NFs layer in DIW and for different concentrations of EtOH. (b) Temporal evolution of the spectrum shift measured for a PA6 NFs sensing layer in real-time. (c) Close up view of the sensing signal evolution where the relative spectrum shift respect DIW is shown for the different EtOH concentrations.

EtOH have been done. Fig. 10 shows the spectrum evolution for one of them. The peak selected to track the sensor response in real-time has been that maximum closer to 600 nm. During the initial minutes, the pumping of DIW over the NFs sensor produces a very significant shift of the spectrum compared to the initial position in air medium. After approximately 30 minutes, once the sensing signal in DIW is stabilized, the sensing test where different concentrations of EtOH are flowed is started. Four EtOH concentrations have been prepared using adequate micropipettes (Eppendorf Research Plus): 40%, 20%, 10% and 5%. Their refractive indices are 1.3583, 1.3469, 1.3395 and 1.3360, respectively [24]. Changes between the different concentrations of EtOH and DIW have been done manually. In order to ensure that the NFs layer is completely filled, the liquid has been flowed during around 10 minutes.

Fig.11 depicts the sensitivity curve determined from the spectral shifts experimentally observed for each EtOH concentration. A notable sensitivity value close to 1025 nm/RIU has been obtained, which is $\sim$2.5$\times$ higher than that theoretically calculated in Fig. 3 ($\sim$ 400 nm/RIU). This higher sensitivity

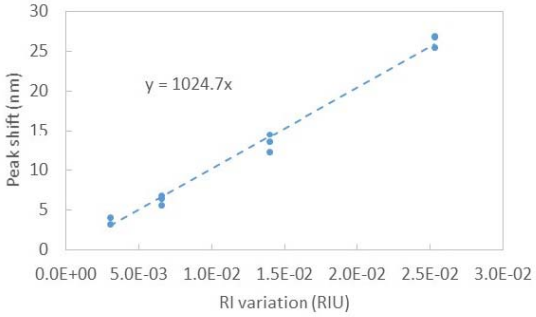

Fig. 11. Sensitivity curve of three different sensing test realized with the same NFs layer covered with a thin gold layer.

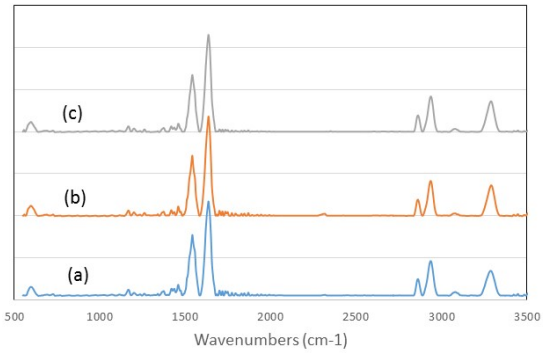

Fig. 12. FTIR spectra of a PA6 NFs layer (a) before performing the experiment, (b) after flowing EtOH and (c) after flowing DIW.

might be determined by the modification of the refractive index of the NFs layer (change in the chemical properties and/or bond densities) during the sensing test, and/or due to a variation in the NFs layer thickness.

VII. Analysis of the Structural Changes in the NFs Layer During a Real-Time and In-Flow Sensing Test

In order to give a response of the higher sensitivity achieved, the first study has consisted on studying the variation of the chemical composition of the NFs layer during the sensing measurement. Comparing the infrared spectra of the NFs layer before and after the sensing measurements (see Fig. 12), all spectra show similar bands with the same intensity. Because of that, we conclude that the chemical composition of the NFs layer was maintained during the sensing experiment.

Secondly, the possibility of having physical changes on the NFs layer after the sensing test has been studied. Fig. 13 shows FESEM images of its micro-morphology for two different positions of the sample: inside and outside the sensing area defined by the flow channel. No significant differences have been observed between the NFs average diameters or density due to the sensing measurement.

Therefore, according to the results exposed, no variation on the NFs layer refractive index due to chemical and/or physical changes is expected.

Assuming that the NFs layer is completely filled by the liquid, and taking into account that the PA6 layer has no variations on its bond densities or refractive index (supposed

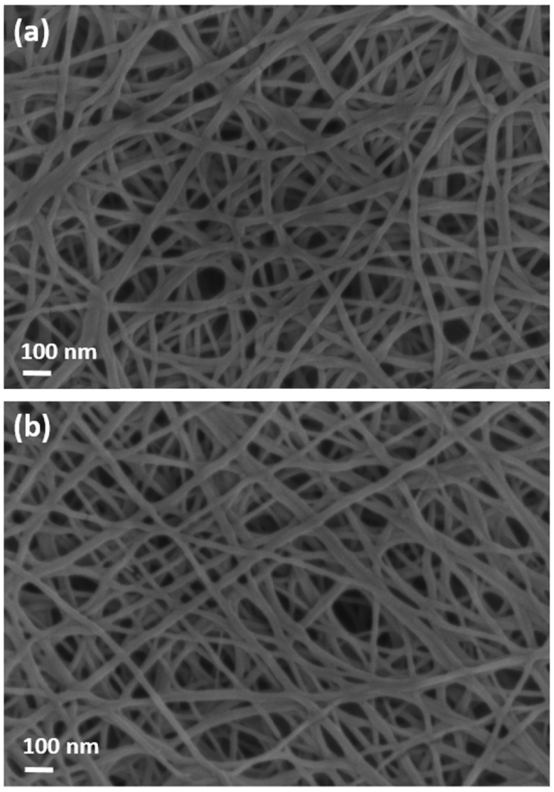

Fig. 13. FESEM images of two different positions of the same NFs layer: (a) within the sensing area and (b) outside the sensing area, but close to it.

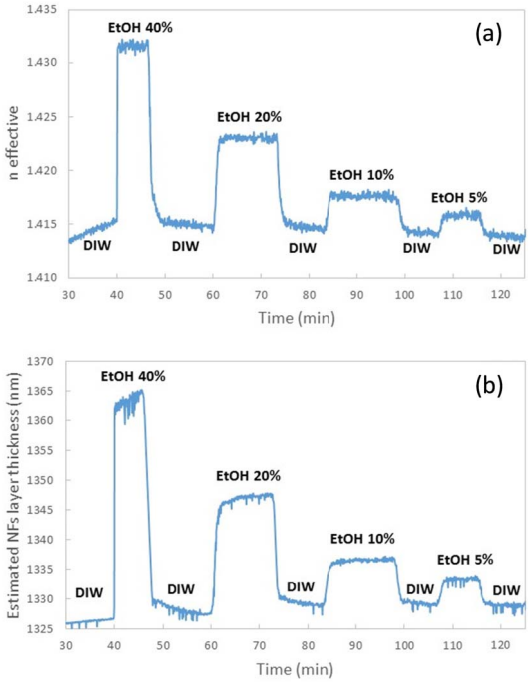

Fig. 14. Estimated (a) effective refractive index and (b) thickness of the NFs layer during the sensing experiment.

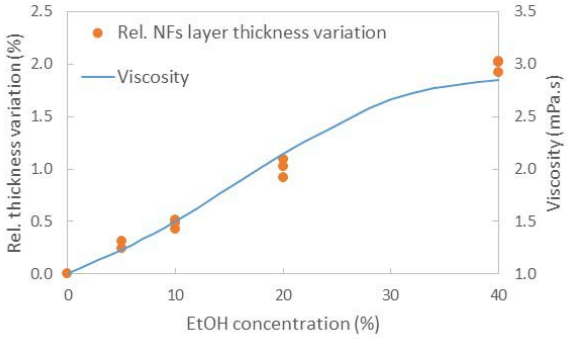

Fig. 15. Relative NFs layer thickness variation and medium viscosity versus the EtOH concentration [24].

independent of wavelength), the non-expected spectrum shift can be justified by the expansion of the NFs layer during the sensing process in real-time. In order to confirm this explanation, we have implemented a Matlab function able to simultaneously determine the effective refractive index and the thickness of the NFs layer throughout the experiment using the measured reflectance spectrum. To this aim, the following equation is used:

$$\lambda = 2hn/m, \tag{1}$$

where λ is the spectral position of a reflectance maximum, h is the NFs layer thickness, n the effective refractive index and m an integer. This equation can be deducted from the reflectance expression given by the Transfer Matrix Method [21]. The maxima positions in the experimental reflectance spectrum are used to estimate by the least square method the values of the parameters in Eq. (1) best fitting those positions. The effective refractive index was calculated as a function of the layer porosity and the refractive index of the medium with the Looyenga model [22].

Fig. 14 shows the estimated effective refractive index of the NFs layer and its thickness depending on the EtOH concentration used during the sensing experiment. According to our simulations, and consistently with the experimental results, the NFs layer modify its thickness during the sensing study. This modification depends on the liquid used during the test, and it increases with the EtOH concentration. In this respect, another parameter that has to be considered in microfluidics-based sensors is the viscosity of the liquids used during the experiments. Viscosity determines the resistance of a liquid to flow and it can be conceptualized as quantifying the frictional force that arises between adjacent layers of fluid that are in relative motion. A large viscosity implies a stronger intermolecular force of attraction within a liquid, giving higher difficulties to be flowed. In this respect, liquids with a higher viscosity produce an expansion of the NFs layer that provides a structure with a higher porosity, which compensates the higher difficulty of the liquid to be flowed.

Fig. 15 shows the relation between the EtOH concentration, its viscosity, and the relative NFs layer thickness variation obtained in the experiments. We can clearly observe that the layer thickness variation follows the same trend than the viscosity of the liquid used during the sensing experiment, thus confirming this relation between NFs expansion and viscosity.

VIII. Conclusion

The potential of new porous optical sensors based on electrospun polyamide NFs layers has been discussed in the

present study. Comparing to other porous substrates, NFs layers have advantages such as: fabrication process suitable for industrialization (since large areas can be fabricated at once with a much reduced production cost), high porosities and a sponge-like structure, allowing a better filling of the sensing structure with the target substances.

One main problem found when using NFs layers as a real-time optical sensor is that the amplitude of the measured FP fringes is very low in an aqueous medium. This limitation has been solved by the deposition of a thin ($\sim$ 3 nm) metal layer. Gold, silver and platinum have been studied because of their high oxidation potential and appropriated reflectance. Among them, gold has been selected due to its high reflectance and its easier and faster deposition method in our laboratory.

An experimental sensitivity much higher than the theoretical one has been obtained when flowing different EtOH concentrations in real-time. It might be determined by the modification of the refractive index of the NFs layer during the sensing experiments, and/or due to a variation in the NFs layer thickness. An FTIR analysis confirms that there are no chemical modifications or the presence of new bond densities. FESEM images show that there are no significant physical differences between the NFs layer inside and outside the sensing area. Because of that, high sensitivities are due to the expansion of the NFs layer. A Matlab program has been developed in order to estimate the effective refractive index of the porous structure and its potential thickness variation. It has been demonstrated that the NFs layer suffers an expansion when flowing liquids in real-time, which has been related to the viscosity of the liquid. Because of that, two parameters can be simultaneously characterized in real-time with an optimized electrospun PA6 NFs layer: the refractive index and the viscosity of the liquid used during the sensing test.

REFERENCES

[1] G. Pickrell, "Special issue of photonic sensors for chemical, biological, and physical parameter detection," *Sensors*, vol. 6, no. 8, pp. 783–784, Aug. 2006.

[2] V. S.-Y. Lin, K. Motesharei, K.-P. S. Dancil, M. J. Sailor, and M. R. Ghadiri, "A porous silicon-based optical interferometric biosensor," *Science*, vol. 278, no. 5339, pp. 840–843, Oct. 1997.

[3] F. Vollmer and S. Arnold, "Whispering-gallery-mode biosensing: Label-free detection down to single molecules," *Nature Methods*, vol. 5, pp. 591–596, Jun. 2008.

[4] J. Villatoro and J. Zubia, "New perspectives in optical crystal fibre sensors," *Opt. Laser Technol.*, vol. 78, pp. 67–75, Apr. 2016.

[5] S. Neethirajan, X. Weng, A. Tah, J. O. Cordero, and K. V. Ragavan, "Nano-biosensor platforms for detecting food allergens—New trends," *Sens. Bio-Sensing Res.*, vol. 18, pp. 13–30, Apr. 2018.

[6] D. L. Presti *et al.*, "Agar-coated fiber Bragg grating sensor for relative humidity measurements: Influence of coating thickness and polymer concentration," *IEEE Sensors J.*, vol. 19, no. 9, pp. 3335–3342, May 2019.

[7] S. K. Khijwania and B. D. Gupta, "Fiber optic evanescent field absorption sensor with high sensitivity and linear dynamic range," *Opt. Commun.*, vol. 152, no. 4, pp. 259–262, Jul. 1998.

[8] C. A. Barrios, "Optical slot-waveguide based biochemical sensors," *Sensors*, vol. 9, no. 6, pp. 4751–4765, Jun. 2009.

[9] H. Ouyang and P. M. Fauchet, "Biosensing using porous silicon photonic bandgap structures," *Proc. SPIE*, vol. 6005, pp. 31–45, Nov. 2005, Art. no. 600508.

[10] F. A. Harraz, "Porous silicon chemical sensors and biosensors: A review," *Sens. Actuators B, Chem.*, vol. 202, pp. 897–912, Oct. 2014.

[11] R. Caroselli, D. M. Sánchez, S. P. Alcántara, F. Prats, L. Torrijos, and J. García-Rupérez, "Real-time and in-flow sensing using a high sensitivity porous silicon microcavity-based sensor," *Sensors*, vol. 17, no. 12, p. 2813, Dec. 2017.

[12] S. Mohammadzadehmoghadam *et al.*, "Electrospinning: Current status and future trends," in *Nano-Size Polymers*, vol. 4. Cham, Switzerland: Springer, 2016, pp. 89–154.

[13] Q. Shi *et al.*, "A facile approach to fabricate porous nylon 6 nanofibers using silica nanotemplate," *J. Appl. Polym. Sci.*, vol. 120, no. 1, pp. 425–433, Apr. 2011.

[14] E. Sapountzi, M. Braiek, J. F. Chateaus, N. Jaffrezic-Renault, and F. Lagarde, "Recent advances in electrospun nanofiber interfaces for biosensing devices," *Sensors*, vol. 17, no. 8, p. 1887, Aug. 2017.

[15] Q. Li *et al.*, "Wire-in-tube IrO_x architectures: Alternative label-free immunosensor for amperometric immunoassay toward α-fetoprotein," *ACS Appl. Mater. Inter.*, vol. 7, no. 40, pp. 22719–22726, Sep. 2015.

[16] X. Mao, W. Tian, T. A. Hatton, and G. C. Rutledge, "Advances in electrospun carbon fiber-based electrochemical sensing platforms for bioanalytical applications," *Anal. Bioanal. Chem.*, vol. 408, no. 5, pp. 1307–1326, Feb. 2016.

[17] M. Mahmoudifard, S. Soudi, M. Soleimani, S. Hosseinzadeh, E. Esmaeili, and M. Vossoughi, "Efficient protein immobilization on polyethersolfone electrospun nanofibrous membrane via covalent binding for biosensing applications," *Mater. Sci. Eng.*, vol. 58, pp. 586–594, Jan. 2016.

[18] C. Dincer, R. Bruch, A. Kling, P. S. Dittrich, and G. A. Urban, "Multiplexed point-of-care testing—xPOCT," *Trends Biotechnol.*, vol. 35, no. 8, pp. 728–742, Aug. 2017.

[19] S. Ponce-Alcántara, D. Martín-Sánchez, A. Pérez-Márquez, J. Maudes, N. Murillo, and J. García-Rupérez, "Optical sensors based on polymeric nanofibers layers created by electrospinning," *Opt. Mat. Express*, vol. 8, no. 10, pp. 3163–3175, 2018.

[20] Q. Yu and X. Zhou, "Pressure sensor based on the fiber-optic extrinsic Fabry–Perot interferometer," *Photonic Sensors*, vol. 1, no. 1, pp. 72–83, Mar. 2011.

[21] R. B. Balili, "Transfer matrix method in nanoopticals," in *Proc. 6th Jagna Int. Workshop Int. J. Mod. Phys., Conf. Ser.*, vol. 17. Singapore: World Scientific, 2012, pp. 159–168. doi: 10.1142/S2010194512008057.

[22] H. Looyenga, "Dielectric constants of heterogeneous mixtures," *Physica*, vol. 31, no. 3, pp. 401–406, 1965.

[23] S. A. A. Oloomi, A. Saboonchi, and A. Sedaghat, "Effects of thin film thickness on emittance, reflectance and transmittance of nano scale multilayers," *Int. J. Phys. Sci.*, vol. 5, no. 5, pp. 465–469, May 2010.

[24] D. R. Lide, "Concentrative properties of aqueous solutions: Density, refractive index, freezing point depression, and viscosity," in *CRC Handbook of Chemistry and Physics*. Boca Raton, FL, USA: CRC Press, 2005, p. 1293.

Salvador Ponce-Alcántara received the M.S. degree in electronic engineering from the University of Granada, Spain, in 2002, and the Ph.D. degree in telecommunication from the Polytechnic University of Madrid, Spain, in 2007. In 2006, he was a Visiting Researcher with the Institute for Energy Technology, Kjeller, Norway. From 2007 to 2011, he was with the Research and Development Department, Isofotón, Málaga, and Pevafersa, Zamora, Spain. In 2011, he was with the Nanophotonics Technology Center, Universitat Politécnica de Valéncia, as a Senior Researcher, where he has been an Assistant Professor since 2015. He holds one utility model and one patent. His research interests include the simulation, characterization, and development of high sensitivity porous silicon photonic sensors.

David Martín-Sánchez received the B.S. degree in telecommunication from the University of Seville, Spain, in 2014, and the M.S. degree in biomedical engineering from the Universitat Politécnica de Valéncia, Spain, in 2016, where he is currently pursuing the Ph.D. degree in telecommunication with the Nanophotonics Technology Center (NTC). Since 2016, he has been a Research Assistant with the Biophotonics Research Group, NTC. His research interests include the design, fabrication, and characterization of photonic sensors based on porous silicon.

Miroslavna Kovylina received the Ph.D. degree in nanotechnology from the University of Barcelona, Spain, in 2011. From 2009 to 2014, she was an Assistant Professor with the University of Barcelona, additionally to carry out her research activity in the fields of nanomagnetism, magnetoresistance, nanoparticles, thin films, and exchange bias. In 2014, she was a Post-Doctoral Researcher with the University of Toronto, Canada. In 2015, she joined the Nanofabrication Group, Nanophotonics Technology Center, Universitat Politécnica de Valéncia. Her research interests include nanofabrication and characterization of the variety of silicon photonic devices and systems.

Ana Pérez-Márquez received the bachelor's degree in chemical engineer from UPV-EHU, Bilbao, in 2008, and the master's degree in innovation and technology management from the Deusto Business School, San Sebastián, in 2009. In 2008, she joined Tecnalia in the Department of Ceramic Materials as a Junior Researcher and worked in the field of nanomaterials focusing on the development of nanofibers based on electrospinning process. She is currently a Researcher with the Aerospace Department, Industry and Transport Division, Tecnalia. Her research interest includes in the field of synthesis and manufacture of micro and nano-structured materials by electrospinning technology for different applications.

Jon Maudes received a bachelor's degree in electronics engineering from UPV-EHU, San Sebastián, in 1999, a Master of smart materials with UPV-EHU, Bilbao, in 2007, and an Industrial Engineer with ETSII-UNED, Madrid, in 2013. In 2002, he joined Inasmet as a Junior Researcher and worked in the fields of metal matrix composite materials with the focus on mechanical properties using foundry techniques. In 2007, he joined the Department of Ceramic Materials and Powder Metallurgy and worked in metallic and ceramic materials with the focus on composite materials with high thermal dissipation capabilities using powder metallurgy processes. Since 2011, he has been a Researcher with the Aerospace Department, Industry and Transport Division, Tecnalia. He is currently involved in the development and characterization of nanostructured materials by electrospinning process and processing of conductive inks for functional printing.

Nieves Murillo received the Ph.D. degree in physical of material from the University of the Basque Country, Spain, in 1997. During her Ph.D. thesis, she was awarded with the Mari Curie Fellowship at the IMEM-CNR Institute, Parma, Italy, and develops part of her research activities in the CSIC Madrid, Spain. She has held a Post-Doctoral position at the Max-Planck Institute, Stuttgart, Germany. She was awarded with the Ramon y Cajal Fellow at Cidetec with successfully assessment of I3 evaluation. She has been the Project Manager with Tecnalia, since 2007. She has participated in over 40 international and national projects and coauthored over 50 scientific publications, including a book chapter. Her citation level is over 280. Her research interests include in two main areas: sensor and actuator development based on smart materials, including optical, piezoelectric, magnetic and superconducting, including the materials design, fabrication, and applications development. She has been a member of organizing committees of three International conferences. She has imparted more than 11 invited talks at international events. Awarded for her research trajectory by the Basque country in 2016. Prize to the Innovation and the endeavor by the Risk and Emergencies Management Conference in 2017.

Jaime García-Rupérez (M'03–SM'16) received the M.S. and Ph.D. degrees in telecommunication from the Universitat Politécnica de Valéncia, Spain, in 2002 and 2008, respectively. He was a Visiting Researcher with the University of Adelaide, Australia, in 2015, and with the National Research Council Canada in 2009. He has been an Associate Professor with the Universitat Politècnica de València since 2005 and a Leader of the Biophotonics Research Group from the Nanophotonics Technology Centre since 2008. His work focuses on the development of integrated photonic biosensing systems for its application in fields as medical diagnosis, environmental control, or biological safety. He is currently the Principal Investigator of two Horizon 2020 European projects focused on the development of high-sensitivity photonic sensing devices for medical diagnosis (H2020-ICT-SAPHELY and H2020-HEALTH-PHOCNOSIS) and of one national project targeting the development of analysis systems based on porous materials for the detection of biological threats (OPTONANOSENS). He has authored over 120 journal and conference publications, one book chapter, and four patents.